Moderate Exercise Prevents Functional Remodeling of the Anterior Pituitary Gland in Diet-Induced Insulin Resistance in Rats: Role of Oxidative Stress and Autophagy

María E. Mercau, Esteban M. Repetto, Matías N. Perez, Camila Martinez Calejman, Silvia Sanchez Puch, Carla V. Finkielstein, and Cora B. Cymeryng

Departamento de Bioquímica Humana (M.E.M., E.M.R., M.N.P., C.M.C., S.S.P., C.B.C.), Facultad de Medicina, Universidad de Buenos Aires, Centro de Estudios Farmacologicos y Botanicos–Consejo Nacional de Investigaciones Cientificas y Tecnicas, Buenos Aires C1121ABG, Argentina; and Integrated Cellular Responses Laboratory (M.E.M., C.V.F.), Department of Biological Sciences and Virginia Bioinformatics Institute, Virginia Tech, Blacksburg, Virginia 24061

A sustained elevation of glucocorticoid production, associated with the establishment of insulin resistance (IR) could add to the deleterious effects of the IR state. The aim of this study is to analyze the consequences of long-term feeding with a sucrose-rich diet (SRD) on *Pomc*/ACTH production, define the underlying cellular processes, and determine the effects of moderate exercise (ME) on these parameters. Animals fed a standard chow with or without 30% sucrose in the drinking water were subjected to ME. Circulating hormone levels were determined, and pituitary tissues were processed and analyzed by immunobloting and quantitative real-time PCR. Parameters of oxidative stress (OxS), endoplasmic reticulum stress, and autophagy were also determined. Rats fed SRD developed a decrease in pituitary *Pomc*/ACTH expression levels, increased expression of antioxidant enzymes, and induction of endoplasmic reticulum stress and autophagy. ME prevented pituitary dysfunction as well as induction of antioxidant enzymes and autophagy. Reporter assays were performed in AtT-20 corticotroph cells incubated in the presence of palmitic acid. *Pomc* transcription was inhibited by palmitic acid-dependent induction of OxS and autophagy, as judged by the effect of activators and inhibitors of both processes. Long-term feeding with SRD triggers the generation of OxS and autophagy in the pituitary gland, which could lead to a decline in *Pomc*/ACTH/glucocorticoid production. These effects could be attributed to an increase in fatty acids availability to the pituitary gland. ME was able to prevent these alterations, suggesting additional beneficial effects of ME as a therapeutic strategy in the management of IR. **(*Endocrinology* 157: 1135–1145, 2016)**

The hypothalamic-pituitary-adrenal (HPA) axis is a key component of the stress response system. Its stimulation by a variety of stress signals results in increased glucocorticoid production by the adrenal cortex. Among other actions, glucocorticoids affect metabolism by stimulating the mobilization of energy stores to cope with increased metabolic demands. However, chronic glucocorticoid excess has deleterious effects and has been associated with an increase in central adiposity, insulin resistance (IR), hyperlipidemia and elevated glucose production (1–3), a similar cluster of abnormalities as those found in the metabolic syndrome. Accordingly, elevations in glucocorticoid activity, either by activation of the HPA axis or by peripheral activation of glucocorticoids

ISSN Print 0013-7227 ISSN Online 1945-7170
Printed in USA

Received September 3, 2015. Accepted December 11, 2015.
First Published Online December 16, 2015

Abbreviations: C-S, control-sedentary; DCFDA, 2′,7′-dichlorofluorescein diacetate; ER, endoplasmic reticulum; HPA, hypothalamic-pituitary-adrenal; IR, insulin resistance; ITT, insulin tolerance test; ME, moderate exercise; NAC, N-acetyl cysteine; NEFA, nonesterified fatty acid; OxS, oxidative stress; PA, palmitic acid; qRT-PCR, quantitative real-time PCR; ROS, reactive oxygen species; SRD, sucrose-rich diet; SRD-E, SRD-exercise; SRD-S, SRD-sedentary; TAG, triacylglycerides.

have been ascribed to the development of metabolic syndrome (4, 5).

Increased consumption of sweet meals or beverages has been linked to the generation of obesity and IR (6–8). Reports on basal activity of the HPA axis in rodent models of IR induced by diet have been controversial as opposing outcomes have been determined (9–11). Recent studies have shown that rats treated with sucrose-rich diets (SRDs) exhibited morphological and functional alterations in the adrenal cortex and a rapid increase in serum glucocorticoid levels associated with the establishment of IR (8). However, the evolution of this parameter over time has not yet been examined.

The present study was designed in order to evaluate the effect of long-term feeding of rats with SRD on ACTH production, a hormone synthesized and released by the pituitary gland that targets the adrenal cortex for glucocorticoid production. To that end, we analyzed pituitary *Pomc* mRNA and ACTH expression levels and the induction of endoplasmic reticulum (ER) stress, autophagy, and oxidative stress (OxS) in pituitary tissue, given that these processes have been associated with the induction of IR (12–14). We also analyzed the effects of a moderate exercise (ME) protocol, a common intervention in patients with IR, applied throughout the duration of the dietary modification. Finally, we determined the effects of palmitic acid (PA), a major component of the nonesterified fatty acid (NEFA) fraction in blood and a parameter altered in SRD-treated animals, on *Pomc*/ACTH production, autophagy, and OxS induction in the murine corticotroph cell line AtT-20.

Materials and Methods

Animals

Adult male Wistar rats (200–250 g) were housed in groups (3 animals/cage) and maintained under controlled conditions of humidity and temperature (21 ± 2°C) and 12-hour light, 12-hour dark cycle. Rats (n = 4–6 per group) were fed a standard chow diet ad libitum and either tap water (Control group) or 30% sucrose in tap water (30% wt/vol, SRD group). Mean caloric intake was monitored every 48 hours throughout the duration of the study (15 wk). All protocols were approved by the Animal Care and Use Committee, Facultad de Medicina, Universidad de Buenos Aires and are in compliance with the Principles of laboratory animal care (National Institutes of Health publication number 85-23, revised 1985).

Insulin tolerance test

An insulin tolerance test was performed on rats after a 4-hour fast. Blood samples were collected from the tail vein at baseline and every 5 minutes after insulin administration (0.8 UI/kg ip, pig regular insulin; Betasint). Serum glucose levels were analyzed with a colorimetric commercial assay (Wiener Labs). The rate constant for plasma glucose disappearance (Kitt) was calculated using the formula $0.693/(t_{1/2})$, and $t_{1/2}$ was obtained from the slope of the least square regression analysis of plasma glucose concentration during the linear phase of decline (15) using GraphPad Prism 6 version 6.0c software (GraphPad Software).

ME protocol

Exercise training sessions consisted of running on an adapted motorized treadmill. In order to prevent possible distress due to the novel environment, animals were placed on the treadmill in "off mode" (10 min/d) 1 week before the initiation of the studies. Training was performed between 8 AM and 12 PM at 13 m/min throughout the study. Training time was adjusted weekly, starting with 1 min/d and increasing gradually (1 min/wk) to 15 min/d on the 15th week after the initiation of the dietary intervention. Selected animals that initially refused to walk were encouraged by gently tapping their backs and subjects reluctant to perform exercise were excluded from the study. The control-sedentary (C-S) group was transported to the experimental room, handled exactly as the experimental animals were and maintained in the turned off treadmill for 5 minutes. The exercise protocol was terminated 48 hours before they were killed.

Tissue and serum samples

Animals were killed by decapitation, between 9 AM and 10 AM, in order to minimize circadian variation among groups and trunk blood was collected. Anterior pituitary glands were excised and tissues were homogenized in 50 mmol/L Na_2HPO_4 (pH 7.4), 0.2 mmol/L EDTA, 100 mmol/L KCl, and 1× protease inhibitor cocktail (Sigma-Aldrich), or TRI reagent (Genbiotech) for RNA extraction.

Biochemical and hormonal measurements

Corticosterone levels were determined in serum samples by RIA after dichloromethane extraction, as described previously (16). The minimal detectable concentration was 0.3 ng/mL and the inter- and intraassay coefficients of variation were 5.9% and 4.9%, respectively. Plasma ACTH levels were determined using Immulite 2000 (Siemens). The minimal detectable concentration was 5 pg/mL, and inter- and intraassay coefficients of variation were 10% and 9.5%, respectively. Fasting serum glucose, triglyceride, and NEFA levels were assessed by colorimetric commercial assays (Wiener Lab and Randox, respectively). Serum insulin levels were determined using a commercial ELISA kit (Alpco Diagnostics Insulin [Rat] Ultrasensitive EIA).

Quantitative real-time PCR (qRT-PCR) assay

Reverse transcription was performed using Moloney Murine Leukemia Virus reverse transcriptase (Life Technologies) as previously described (17). Amplifications by real-time PCR were carried out in a Rotor-Gene 6000 Corbett Life Science Real Time Thermal Cycler (Corbett Research) and quantified with the Rotor Gene 6000 Series Software (version 1.7 Build 40). Primer oligonucleotide sequences used in this study were as follows: for *Pomc* (encodes for proopiomelanocortin [POMC]) Forward (F), 5′-CCTCACCACGGAAAGCA-3′ and Reverse (R), 5′-TCAAGGGCTGTTCATCTCC-3′; for *Grp78* (encodes for binding immunoglobulin protein) F, 5′-CCGAGTGACAGCTGAAGACA-3′ and R, 5′-GCGCTCTTTGAGCTTTTTGT-3′;

for *Dnajc3* (encodes for DnaJ [Hsp40] homolog, subfamily C, member 3; hereafter mentioned as $p58^{IPK}$) F, 5′-ATTAAAGCATACCGAAAGTTAGCAC-3′ and R, 5′-AGAGGGTCTTCTCCGTCATCAAA-3′ and for *Actb* (encodes for β-actin) F, 5′- CCACACCCGCCACCAGTTC-3′ and R, 5′-GACCCATTCCCACCATCACACC-3′. Gene expression levels were normalized to *Actb* as an internal control, using the ΔΔCt relative quantification method (18).

Immunoblot analysis

Pituitary homogenates were resolved by SDS-PAGE and transferred to polyvinylidinefluoride membranes in a Trans-Blot Semi-Dry system (Bio-Rad Laboratories, Inc). Membranes were blocked, probed and developed as described previously (17). Chemiluminescence was detected with the ImageQuant Imaging System (GE Healthcare) and quantification was performed using ImageJ software (National Institutes of Health). For further details on antibodies see Table 1.

Cells and culture conditions

The mouse ACTH-secreting pituitary adenoma cell line, *AtT-20/D16v-F2* (hereafter mentioned as AtT-20) (19), was obtained from the American Type Culture Collection. AtT-20 cells were maintained in DMEM (Invitrogen) supplemented with 10% heat-inactivated fetal bovine serum, 100-U/mL penicillin, 100-μg/mL streptomycin, and incubated at 37°C and 5% CO_2. All treatments were performed in serum-free DMEM. Cell viability, assessed by the trypan blue exclusion method, was calculated as % ratio of viable cells (unstained) to total cells. None of the treatments described in this study affected cell viability assessed by this method. PA stock solution was prepared by dissolving PA (Sigma-Aldrich) in ethanol to a final concentration of 50 mmol/L (12.8 mg/mL). On the day of the experiment, PA was conjugated to fatty acid-free BSA (Sigma-Aldrich) by mixing PA with 4% BSA wt/vol in serum-free DMEM at 37°C for 1 hour, before use. Different concentrations (0.25–1 mmol/L) of PA were added to cultures. Control cultures received medium containing 4% BSA.

Transfections and reporter assays

AtT-20 cells were seeded in 96-well plates (10^4 cells/well) and transfected using Lipofectamine 2000 (Invitrogen), *Pomc*-pGL3 (0.18 μg/well; Addgene), and pCMV-*β-gal* (0.02 μg/well) following manufacturer's instructions. Luciferase activity was determined using the Steady-Glo Luciferase Assay System (Promega Corp). Values were normalized to β-galactosidase activity. In other experiments, AtT-20 cells (5×10^5 cells/well) were transfected with pmRFP-LC3 expression plasmid (1.44 μg/well; Addgene). pmRFP-LC3 expresses a fusion protein of monomeric red-fluorescence protein and mouse LC3, a widely used marker for autophagosomes. Two days after transfection, cells were treated accordingly, and LC3-RFP fluorescence was visualized by epifluorescence microscopy (BX50; Olympus). Images were analyzed with Image-Pro Plus (Media Cybernetics, Inc). *Pomc*-pGL3 was provided by Domenico Accili (Addgene NCBI number 17553) (20), and pmRFP-LC3 was kindly supplied by Tamotsu Yoshimori (Addgene NCBI number 21075) (21).

Detection of intracellular reactive oxygen species (ROS) generation

Intracellular ROS generation was measured in AtT-20 cells using the nonfluorescent probe 2′,7′-dichlorofluorescein diacetate (DCFDA) (Molecular Probes; Invitrogen). Upon uptake by the cells DCFDA is hydrolyzed by esterases and rapidly oxidized by intracellular ROS to the fluorescent DCF. After treatments, cells were loaded with 10μM DCFDA in 1× PBS for 60 minutes at 37°C and processed as described previously (17). Fluorescence intensity (excitation, 485 nm; emission, 535 nm) was determined in a multimode microplate reader, FLUOstar Omega (BMG Labtech). ROS levels were normalized to total protein content and expressed in arbitrary units.

Statistical analysis

All values are expressed as mean ± SEM of n experiments. Differences between groups were analyzed by 2-tailed unpaired Student's *t* test or by one-way ANOVA, as appropriate. When the ANOVA yielded significant differences ($P < .05$), post hoc comparisons (Dunnett or Tukey's tests) were made to determine

Table 1. Antibody Table

Peptide/ Protein Target	Antigen Sequence (If Known)	Name of Antibody	Manufacturer, Catalog Number, and/or Name of Individual Providing the Antibody	Species Raised in; Monoclonal or Polyclonal	Dilution Used
ACTH		ACTH antibody (SPM333)	SCBT, sc-52980	Mouse; mAb	1:1000 (WB), 1:2000 (IF)
Hemeoxygenase-1		HO-1 polyclonal antibody	Enzo Life Sciences, ADI-SPA-896	Rabbit; pAb	1:1000
Catalase		Human/mouse/rat catalase antibody	R&D Systems, AF3398	Goat; pAb	1:250
p62 (SQSTM1)		SQSTM1 antibody (H-290)	SCBT, sc-25575	Rabbit; pAb	1:500
LC-3		LC3A/B (D3U4C) XP rabbit mAb	Cell Signaling Technology, 12741	Rabbit; mAb	1:1000
Actin		Actin antibody (I-19)	SCBT, sc-1616	Rabbit; pAb	1:1000
Antirabbit HRP conjugated		Goat antirabbit IgG (H + L)-HRP conjugate	Bio-Rad Laboratories, 170-6515	Goat; IgG	1:10 000
Antimouse HRP conjugated		Antimouse IgG, HRP-linked antibody	Cell Signaling Technology, 7076	Horse; IgG	1:2000
Antigoat HRP conjugated		Goat IgG horseradish peroxidase-conjugated antibody	R&D Systems, HAF017	Rabbit; IgG	1:2000
Antimouse Cy3 conjugated		Cy3 AffiniPure goat antimouse IgG (H + L)	Jackson ImmunoResearch, 115-165-003	Goat; IgG	1:500

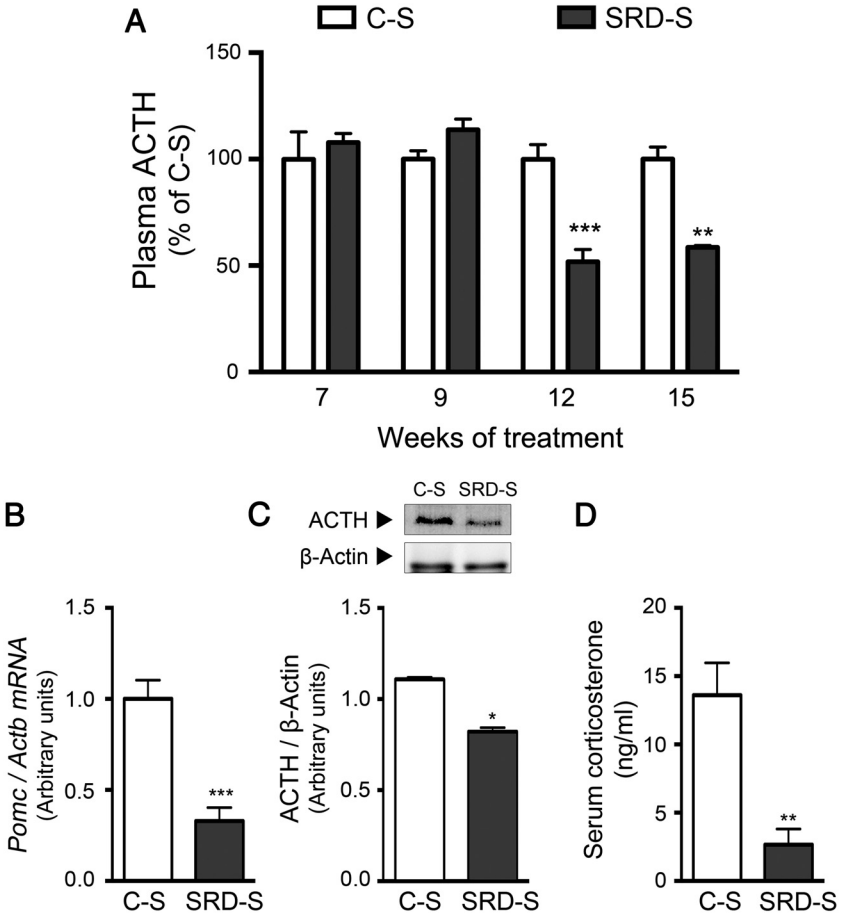

Figure 1. Long-term treatment with SRD impairs HPA axis activity in rats. A, Plasma ACTH levels were determined weekly in C-S and SRD-S rats using a chemiluminescent immunoassay. Pituitary parameters were assessed in tissues after 15 weeks of SRD treatment: (B) *Pomc* mRNA levels, as determined by qRT-PCR, and (C) a representative image of ACTH expression levels as determined by immunoblotting and quantification of results. D, Serum corticosterone levels were assessed by RIA in C-S and SRD-S rats. Values are expressed as mean ± SEM, n = 5; *, $P < .05$; **, $P < .01$; and ***, $P < .001$ vs respective C-S, by unpaired Student's *t* test.

the statistical difference between groups. All calculations were performed using GraphPad Prism 6 version 6.0c (GraphPad Software).

Results

In the present study, we analyzed the effect of feeding rats a SRD, on the pituitary production of ACTH. Consequently, we monitored plasma ACTH levels in animals from C-S and SRD-sedentary (SRD-S) groups, from the seventh week up to the 15th week of treatment. No significant differences between groups were observed in either the seventh or the ninth week of treatment. However, significantly lower plasma ACTH levels were determined in SRD-S animals from then on (Figure 1A). The next experiments were performed in rats after 15 weeks of SRD treatment. In agreement with plasma ACTH results, decreased pituitary *Pomc* mRNA (Figure 1B) and ACTH protein levels (Figure 1C) were determined in SRD-treated rats. In addition, lower serum corticosterone levels were also observed in SRD-treated animals compared with C-S (Figure 1D).

Our results show that rats fed SRD for 15 weeks exhibited significantly increased fasting levels of several serum parameters (glucose: C-S, 98.7 ± 5.9 and SRD-S, 139.7 ± 4.3 mg/dL; $P < .001$, insulin: C-S, 1.02 ± 0.06 and SRD-S, 1.84 ± 0.18 ng/mL; $P < .01$, NEFA: C-S, 0.84 ± 0.01mM and SRD-S, 1.00 ± 0.04mM; $P < .01$, and triacylglycerides (TAG): C-S, 93.2 ± 13.3 and SRD-S, 173.2 ± 19.3 mg/dL, $P < .05$). Tissues are, thus, exposed to increased levels of nutrients whose metabolism may lead to the formation of potentially deleterious mediators. Either glucotoxicity or lipotoxicity could then induce cellular defense responses. As noted above, induction of OxS, ER stress, and autophagy have been associated with diet-induced IR in several tissues. In agreement, analysis of pituitary glands obtained from rats treated with SRD for 15 weeks indicated increased expression levels of antioxidant enzymes (Figure 2, A and B), and changes in markers of ER stress (Figure 2, C and D) and autophagy (Figure 2, E and F) that were consistent with the induction of these processes. Apoptosis, evaluated by Poly ADP ribose polymerase cleavage, was undetectable in our experimental conditions (data not shown).

We then determined the effects of ME on the pituitary dysfunction observed in SRD-S rats. Briefly, control or SRD-treated rats were subjected to a ME protocol for 15 weeks (as described in Materials and Methods). Data indicate that mean individual caloric intake, fat depots, or body weight remained unchanged in ME-treated SRD groups (SRD-exercise [SRD-E]) compared with sedentary controls (C-S) (Table 2). In addition, ME had no effect on fasting serum glucose and triglyceride concentration, or on insulin sensitivity but significantly prevented the increase in serum NEFA levels triggered by SRD (Figure 3, A–D).

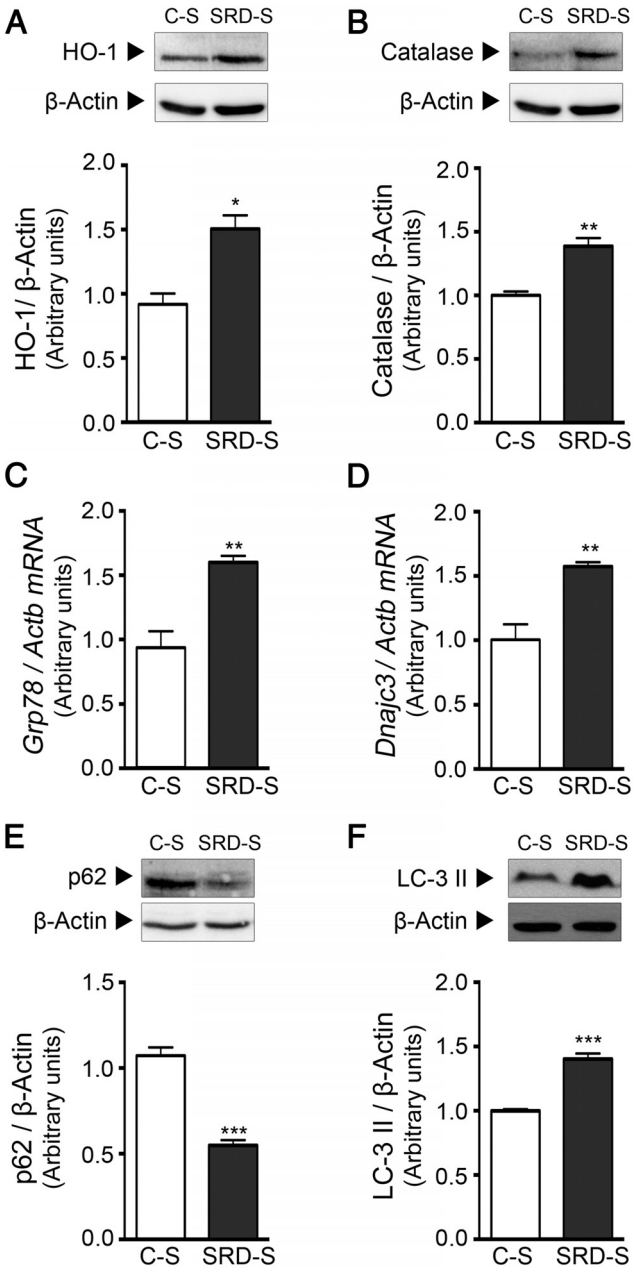

Figure 2. Pituitary antioxidant enzyme expression, ER stress, and autophagy markers are induced by SRD after 15 weeks of treatment. Proteins were obtained from C-S and SRD-S groups. Representative immunoblots and quantification of results for (A) hemeoxygenase-1 and (B) catalase. mRNA levels, assessed by qRT-PCR, for (C) *Grp78* and (D) *Dnajc3* ($p58^{IPK}$). Representative immunoblots and quantification of results for (E) p62 and (F) LC3-II. Values are mean ± SEM, n = 3; *, $P < .05$; **, $P < .01$; and ***, $P < .001$ vs C-S, by unpaired Student's *t* test.

Regarding pituitary parameters, ME prevented the induction of antioxidant enzymes and autophagy observed in SRD-treated rats but was unable to block the generation of ER stress induced by the modification of the diet (Figure 4, A–F). Interestingly, ME prevented the decrease of *Pomc* mRNA in the pituitary gland (Figure 5A), plasma ACTH (Figure 5B) and basal serum corticosterone levels (Figure 5C) in SRD-treated rats. Noteworthy, neither SRD nor ME, alone or combined, modified the number of corticotroph cells, evaluated by immunofluorescence of ACTH-positive cells in paraffin embedded pituitary glands (quantification is shown in Supplemental Figure 1). In addition, hematoxylin-eosin staining did not show evidence of changes in pituitary morphology between groups (Supplemental Figure 2).

In order to analyze the effect of induction of autophagy or OxS on *Pomc*/ACTH synthesis in pituitary corticotrophs, we transiently transfected AtT-20cells with a *Pomc*-promoter driven reporter plasmid (*Pomc*-pGL3) and treated the cells with the autophagy inductor, rapamycin or the OxS generator, H_2O_2. Our results indicate that both treatments induced a significant decrease in *Pomc* reporter activity (Figure 6, A and B).

The inverse correlation between plasma NEFA concentration and pituitary POMC/ACTH expression levels detected in vivo prompted us to determine the effects of PA (C16:0), a major component of NEFA, on pituitary corticotroph cells AtT-20. Our results showed that PA treatment induced a decrease in both luciferase activity of *Pomc*-pGL3and endogenous POMC protein levels (Figure 7, A and B). Further studies were performed on AtT-20 cells that were transfected with pmRFP-LC3 expression plasmid and treated with PA. Distinct red fluorescence puncta, associated with autophagosome formation, were detected 24 hours after lipid treatment (Figure 7C, left panel). Quantification of total fluorescence intensity of different samples yielded no significant changes (Figure 7C, right panel). The increase in LC3-II levels was further confirmed by immunoblotting (Figure 7D). PA also induced ROS generation as judged by increasing DCF fluorescence (Figure 7E). We then determined that pharmacologic inhibitors of autophagy (LY294002, a phosphatidylinositol-3-kinase inhibitor) and OxS (N-acetyl cysteine [NAC]) prevented the decrease in *Pomc*-pGL3 activity (Figure 7F) and POMC endogenous protein levels (Figure 7H) in PA-treated AtT-20 cells. In addition, LY294002 did not prevent PA-induced ROS generation (Figure 7G), whereas NAC prevented autophagy induction (LC3 cleavage) by PA treatment (Figure 7H), suggesting a causal effect of OxS on autophagy.

Discussion

We have previously demonstrated that rats rendered insulin resistant by the administration of a SRD showed elevated serum corticosterone levels after 7 weeks of treatment (8). Increased production or local activation of glucocorticoids may add to the factors that contribute to ag-

Table 2. Biometric Data From Sedentary and Exercised Animals Fed SRD or Control Diets

	C-S	SRD-S	C-E	SRD-E
Body weight (g)	302.8 ± 16.6	367.4 ± 12.2[a]	301.5 ± 7.8	368.2 ± 16.9[a]
Retroperitoneal fat (g)	11.8 ± 0.8	26.9 ± 1.4[c]	11.2 ± 0.9	27.0 ± 2.3[c]
Visceral fat (g)	11.4 ± 0.7	21.0 ± 0.9[b]	12.5 ± 0.9	18.7 ± 2.7[a]
Epididymal fat (g)	11.6 ± 0.9	21.0 ± 0.2[c]	12.0 ± 0.5	16.8 ± 2.5[a]
Mean caloric intake (kcal/rat/day)	142.6 ± 2.7	206.0 ± 6.4[c]	143.0 ± 3.5	199.3 ± 5.7[c]

Mean caloric intake was calculated every 2 days throughout the experiment. Total body weight and fat depots weight correspond to the experiment's endpoint. Values are presented as mean ± SEM, n = 5.

[a] $P < .05$ vs C-S. ANOVA followed by Tukey's post hoc test.

[b] $P < .01$ vs C-S. ANOVA followed by Tukey's post hoc test.

[c] $P < .001$ vs C-S. ANOVA followed by Tukey's post hoc test.

gravate the somatic and metabolic disorders that characterize the IR syndrome. However, whether this increased production of glucocorticoids is sustained over time remains unknown. To our knowledge, this is the first report showing that prolonged consumption of a SRD results in a significant decrease in both the production and release of ACTH and corticosterone, by effects exerted at pituitary level. Down-regulation of glucocorticoid levels would ultimately decrease the metabolic stress induced by glucocorticoid excess attenuating the deleterious effects associated with this condition.

Our results show a decrease in *Pomc* expression levels and ACTH production by the pituitary gland (and a concomitant reduction in serum glucocorticoid levels) several weeks after the establishment of IR. This impairment of pituitary function could be associated with an increased generation of ROS and the induction of ER stress and autophagy, given that changes in markers of those processes were readily detected. Interestingly, the application of a ME protocol to SRD-treated animals prevented the induction of antioxidant enzymes and autophagy, as well as the decrease in pituitary ACTH synthesis and release. In

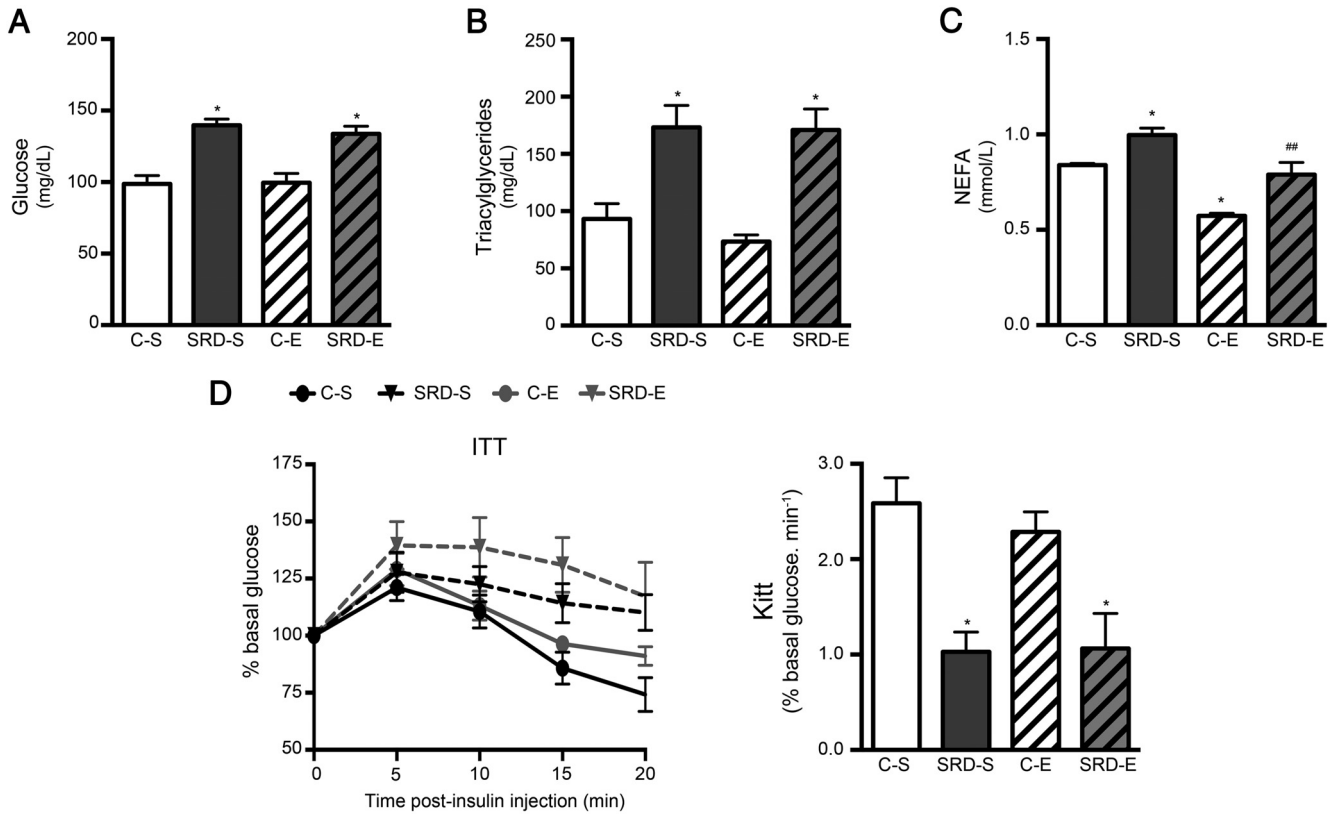

Figure 3. ME attenuates the increase in NEFA levels in serum of SRD-treated rats. Animals were randomly assigned to the next 4 groups: C-S, SRD-S, control-exercise (C–E), and SRD-E, and treated for 15 weeks with SRD and/or ME as described in Materials and Methods. Glucose (A), TAG (B), and NEFA (C) levels were determined in serum. D, An ITT was performed on the 15th week of treatment on 4-hour-fasted animals. Left panel shows the decrease in serum glucose levels after injection with 0.8-IU/kg insulin, and glucose disappearance rates (Kitt) are presented on the right. Values are expressed as mean ± SEM, n = 5; *, $P < .05$ vs C-S; and ##, $P < .01$ vs SRD-S; ANOVA followed by Tukey's test.

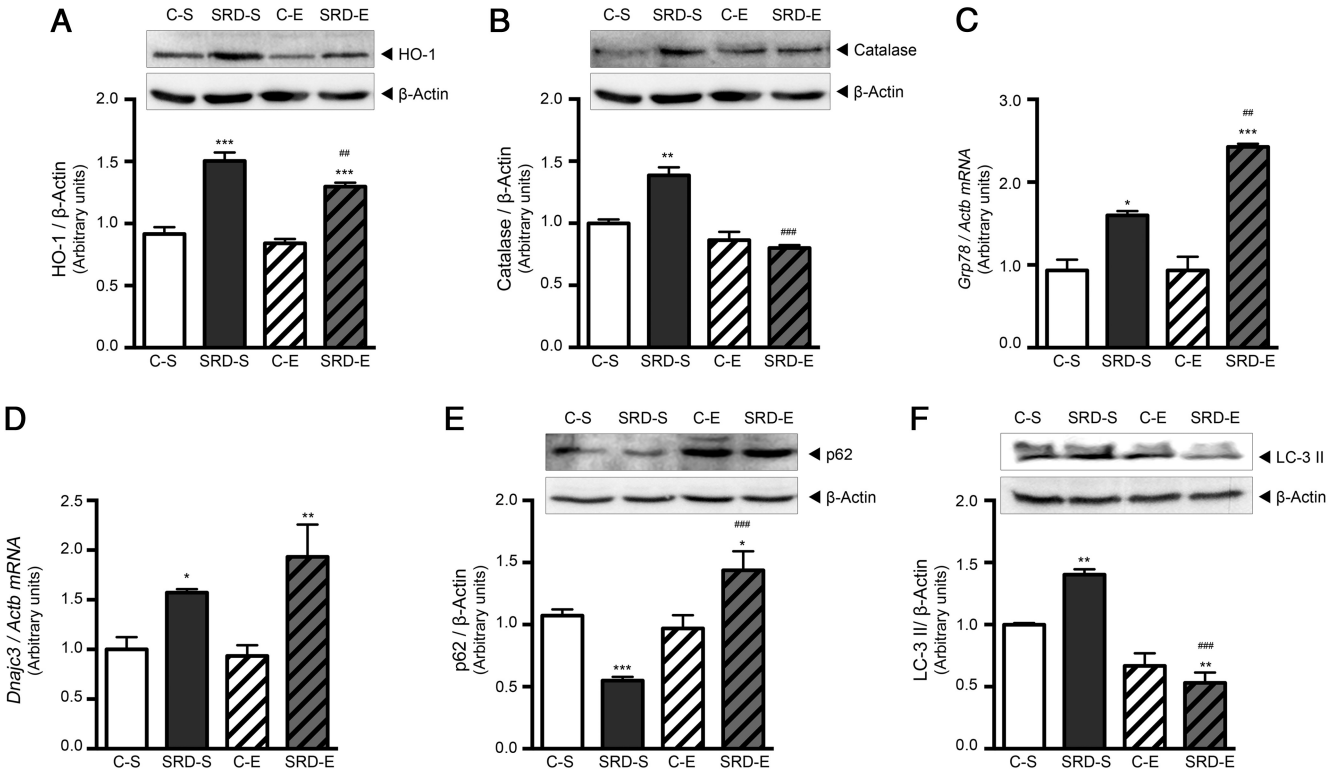

Figure 4. ME prevents changes in antioxidant enzyme levels and autophagy without affecting ER stress. Pituitary glands from animals treated as described in the legend of Figure 3 were examined. Representative immunoblot images and the corresponding densitometric analysis for (A) HO-1 and (B) catalase. Relative mRNA levels of 2 ER stress markers, (C) *Grp78* and (D) *Dnajc3* (*p58*^{IPK}). Protein levels of 2 autophagy markers, (E) p62 and (F) LC3-II, were assessed by immunoblotting (upper panels) and plotted above the densitometric analysis (bar graphs). Values are expressed as mean ± SEM, n = 3; *, $P < .05$; **, $P < .01$; and ***, $P < .001$ vs C-S; and $^{\#\#}$, $P < .01$; $^{\#\#\#}$, $P < .001$ vs SRD-S; ANOVA followed by Tukey's test.

this sense, we hypothesized that those processes could be involved in the observed decline in pituitary function.

The effect of diet-induced obesity on the activity of the HPA axis has been the subject of previous studies (10, 11, 22, 23). However, a comprehensive analysis of these reports does not generate conclusive results. Disparate outcomes were attributed to different experimental protocols, species or diets, among other factors (9). In agreement with our results, decreased glucocorticoid levels were determined in mice and pigs fed high-fat diets for several weeks (23, 24).

Generation of OxS in different tissues of animals with diet-induced IR has been described previously (13, 25–27). An oversupply of nutrients to the cells can result in ROS generation, mainly by the mitochondrial electron transport chain leaking species of oxygen not fully reduced. Other sources of ROS include plasma membranes, peroxisomes, the cytosol and the ER (28). Our results show the induction of antioxidant enzymes that could be the result of increased ROS generation in pituitary cells. Among other consequences, an unbalance ROS production could lead to mitochondrial dysfunction, loss of DNA integrity, protein misfolding and ER stress (29). ER stress has been also associated with obesity and IR generation (12, 30). In particular, induction of ER stress in fructose fed rats has been reported in adipose and liver tissues (31, 32).

ER stress-induced response involves expansion of the ER protein folding capacity and reduction of the load of new proteins by a general inhibition of translation. Misfolded proteins could then be eliminated by the proteosomal pathway, but autophagy induction has also been associated with the generation of ER stress (14, 33, 34). Autophagy is generally considered as a protective mechanism. Depending on the context, autophagy could counter balance ER stress, enhancing cell survival, or promote cell death. In this regard, pharmacological induction of autophagy in diet-induced IR has been shown to reduce ER stress and apoptosis in pancreatic β-cells (35). Our results also indicate the induction of ER stress and autophagy in the pituitary glands of SRD-treated rats. In our model, induction of these cellular processes correlates with the impairment of POMC/ACTH production, raising the possibility that both observations could be related.

Exercise has been strongly recommended to obese and diabetic patients for its widely acknowledged positive impact on insulin sensitivity (36). In rats, exercise has been shown to prevent the effects of SRD on insulin action,

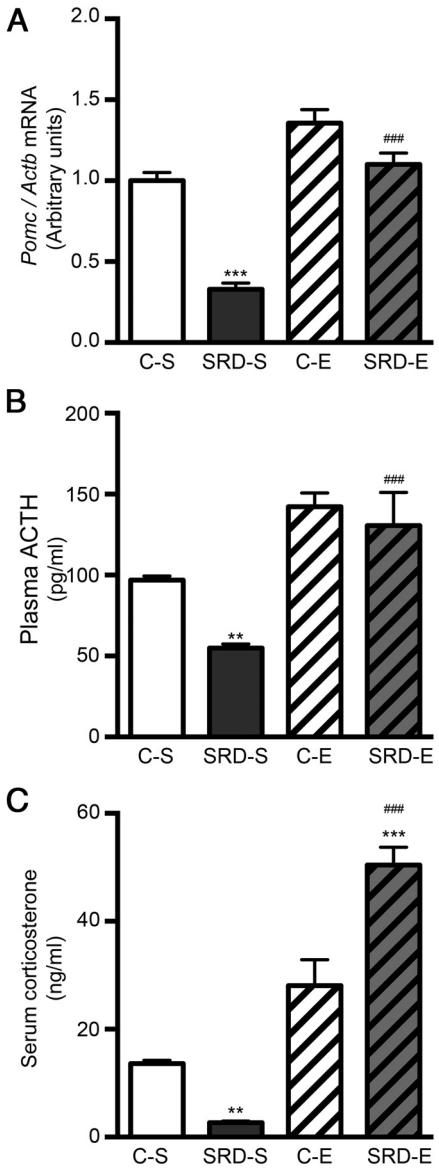

Figure 5. Exercise prevents changes in pituitary *Pomc* and systemic ACTH and corticosterone levels in SRD-treated animals. Blood samples and pituitary tissues obtained from rats treated as in Figure 3 were analyzed. *Pomc* mRNA (A) and plasma ACTH levels (B) and serum corticosterone concentrations (C). Values are expressed as mean ± SEM, n = 5; **, $P < .01$; and ***, $P < .001$ vs C-S; and ###, $P < .001$ vs SRD-S; ANOVA followed by Tukey's test.

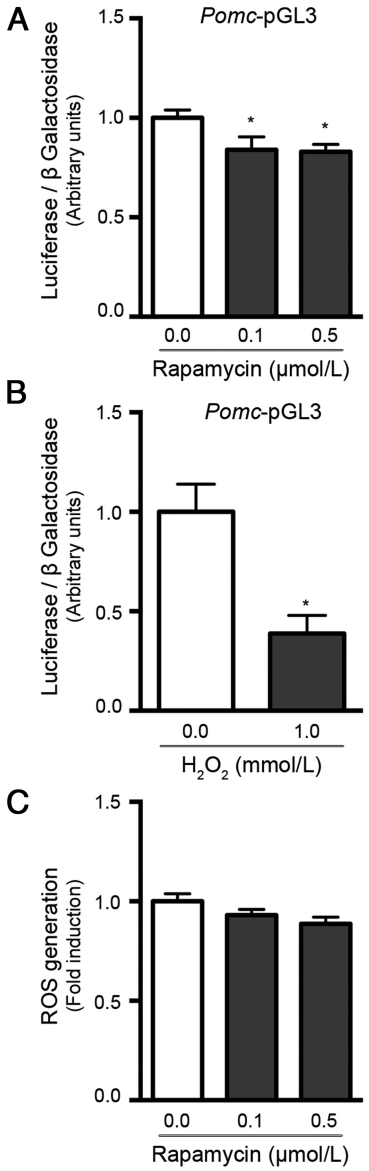

Figure 6. ROS and autophagy induction decrease POMC expression levels in the corticotroph cell line AtT-20. Cells were treated with (A) the indicated concentrations of the autophagy inductor rapamycin for 24 hours or (B) 1 mmol/L H_2O_2 for 3 hours. Luciferase activity was determined in cells transiently transfected with the reporter plasmid *Pomc*-pGL3. Values are expressed as mean ± SEM, n = 4; *, $P < .05$ vs respective control; ANOVA followed by Dunnett's post hoc test (A and C) and Student's *t* test (B).

improving glucose uptake by muscle tissues (37). As for the activity of the HPA axis, normalizing effects exerted mainly at adrenocortical level, have been ascribed to exercise in Zucker male diabetic fatty rats (38). In our experimental setting, the results of the insulin tolerance test (ITT) suggested that IR was established in rats from both SRD-treated groups (SRD-S and SRD-E) after 15 weeks of treatment. This lack of effect of exercise on insulin sensitivity could be due to the fact that our ME protocol was much less intense than others described in the bibliography, as extreme care was taken to minimize external stressful stimuli considering that the activity of the HPA axis was under study. Regardless, ME prevented the decrease in *Pomc* mRNA, plasma ACTH and serum corticosterone levels observed in sedentary animals fed a SRD for 15 weeks, suggesting that at least in the time frame of our study, ME prevents the generation of pituitary dysfunction by a mechanism that does not affect the development of IR, as shown by the results of the ITT test.

Noteworthy, none of the treatments (SRD or ME alone or combined) modified the number of corticotrophs or the

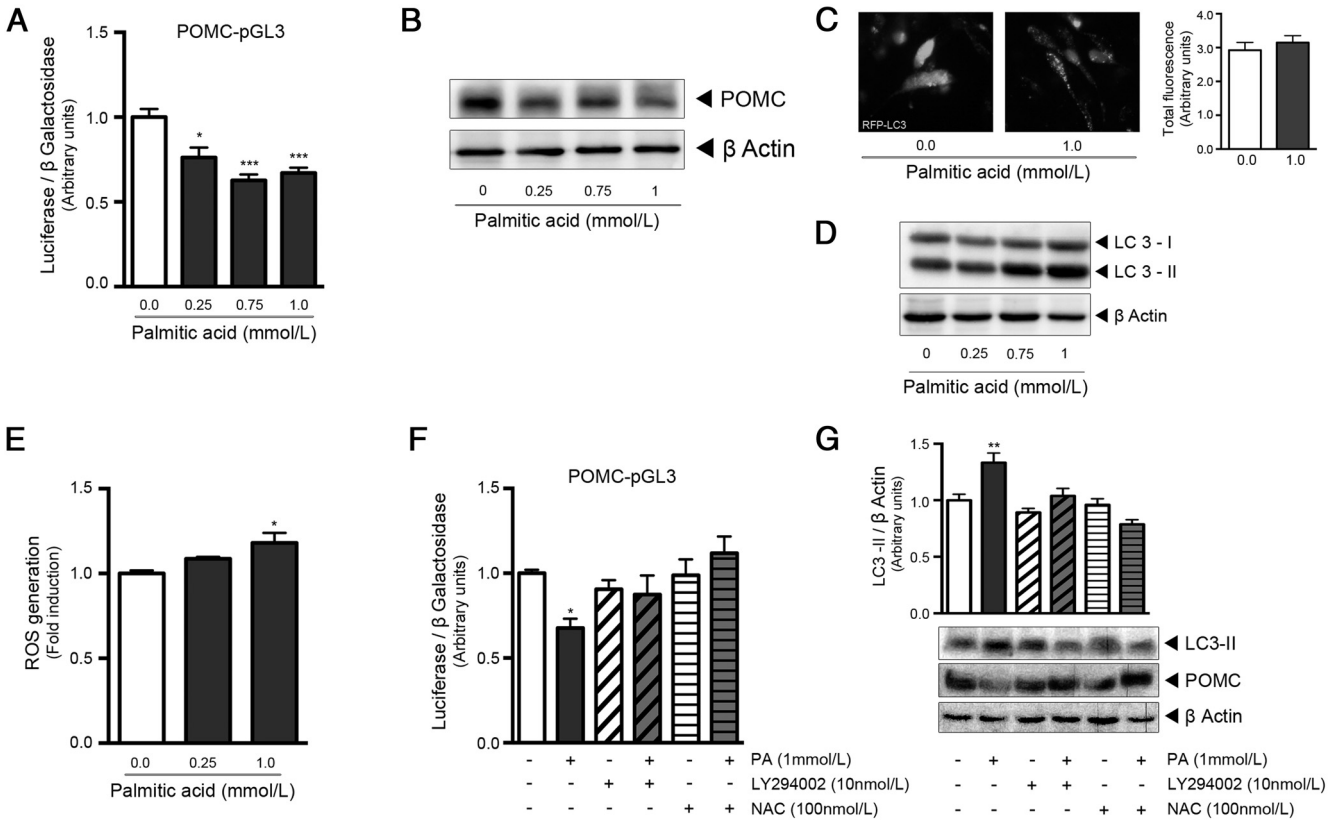

Figure 7. OxS and autophagy mediate the impairment of POMC expression by PA in AtT-20 cells. Effect of PA treatment on (A) luciferase activity of the reporter plasmid *Pomc*-pGL3 and (B) endogenous POMC protein levels, as determined by immunoblot. C, Cells were transfected with pmRPF-LC3 and autophagy was assessed by puncta formation in PA-treated AtT-20 cells and (D) by endogenous LC-3 conversion, determined by immunoblotting. E, Effect of PA on ROS generation, as determined by DCFDA fluorescence. F, *Pomc*-pGL3 luciferase activity in PA-treated AtT-20 cells with or without autophagy inhibitor LY294002 (10 nmol/L) or antioxidant NAC treatment (NAC) (100 nmol/L). G, Effect of autophagy inhibitor LY294002 or antioxidant NAC treatment on PA-induced ROS generation, determined by DCFDA fluorescence. H, LC3-II processing and endogenous POMC expression in PA-treated cells, coincubated with LY294002 or NAC. Values are expressed as mean ± SEM, n = 4; *, $P < .05$; **, $P < .01$; and ***, $P < .001$ vs control; ANOVA followed by Dunnett's post hoc test.

morphology of the pituitary glands in any of the experimental groups.

Because exercise also blocked the induction of antioxidant enzymes and autophagy, with no effect on ER stress markers, we hypothesized that either ROS generation, autophagy or both processes could be involved in the inhibitory effect of SRD on pituitary function. Given the inherent complexity of animal models we tested this hypothesis in a corticotroph cell line (AtT-20). In this cell line we demonstrated that inductors of OxS or autophagy, as hydrogen peroxide and rapamycin, respectively, decreased *Pomc*-driven luciferase activity, suggesting that both processes could be involved in the modulation of *Pomc* expression levels.

Generation of IR in muscle and adipose tissue has been associated with supraphysiological NEFA levels via the production of DAG, ceramides and OxS (39, 40). In our experiments we found that SRD treatment significantly increased NEFA levels. Interestingly, ME prevented this alteration, whereas it did not affect body weight, peripheral insulin sensitivity, or serum glucose or TAG concentration, as stated above. Regarding the fatty acid composition of the NEFA fraction, recent studies have demonstrated an increase in the levels of PA in male Wistar rats fed with SRD for 16 weeks (41). Conversely, it was previously demonstrated that acute infusion of PA, or intralipid, decreases basal ACTH and glucocorticoid levels in male Wistar rats and humans, respectively (42, 43).Collectively, these evidences led us to hypothesize that elevated PA levels could trigger a decrease in POMC/ACTH generation by inducing OxS and autophagy in the pituitary gland of SRD-treated rats. Accordingly, we then demonstrated that PA treatment significantly inhibited POMC expression while inducing ROS generation and autophagy in AtT-20 cells. Pharmacological inhibition of each process prevented the PA-dependent inhibition of *Pomc* transcription, thus suggesting their involvement in the effect. Additionally, as inhibition of autophagy did not prevent ROS generation, whereas antioxidant treatment precluded autophagy induction, a causal relationship

between ROS generation and autophagy induction by PA treatment is suggested. Yan et al also demonstrated the induction of autophagy by OxS in Goto-Kakizaki rats (44).

Our results showed a decrease in *Pomc* mRNA levels in pituitary glands obtained from rats treated with SRD for 15 weeks. An impairment in *Pomc* mRNA transcription (by factors affecting the basal transcription rate or the negative feedback by glucocorticoids), as observed in PA-treated corticotroph cells, or a decrease in the mRNA stability could account for the lower *Pomc* mRNA levels observed in our experiments. Additional changes in the pituitary proteolytic activity of POMC-specific convertases, as reported in the hypothalamus of rats fed a high-fat diet (45) or other posttranslational mechanisms cannot not be discarded based on present results.

In summary, our results demonstrate that SRD induced a decrease in basal POMC/ACTH expression levels and blood ACTH and corticosterone concentrations after several weeks of treatment. A ME intervention, applied from the beginning of the dietary modification, prevented the pituitary dysfunction and also the generation of ROS and autophagy induced by excess nutrient availability. Our in vitro studies also demonstrate that PA treatment of corticotroph cells can reproduce the decline in *Pomc* transcription via a mechanism that involves OxS-induced autophagy.

Although the decline in glucocorticoid production could attenuate many of the characteristics of the IR state, care should be taken to prevent adrenal insufficiency, a potentially dangerous condition that leads to an inadequate response to stressful stimuli. In this sense, ME has proven to have a beneficial preventive effect. Future studies will focus on ME as a therapeutic strategy once IR has been established.

Acknowledgments

We thank Dr J. J. Lopez for his assistance with the histological analysis of pituitary tissue.

Address all correspondence and requests for reprints to: Cora B. Cymeryng, PhD, Departamento de Bioquímica Humana, Facultad de Medicina, Universidad de Buenos Aires, Paraguay 2155, 5° Piso, Buenos Aires C1121 ABG, Argentina. E-mail: cymeryng@fmed.uba.ar.

This work was supported by the Agencia Nacional de Promoción de Ciencia y Tecnología Grant ANPCyT PICT 2008 N°1034, the Consejo Nacional de Investigaciones Científicas y Técnicas Grant CONICET PIP 11220120100257, the Universidad de Buenos Aires Grant UBACyT 20020130100115BA (to C.B.C.), and the National Sciences Foundation Grant MCB-1517298 (to C.V.F.).

Disclosure Summary: The authors have nothing to disclose.

References

1. **Peeke PM, Chrousos GP.** Hypercortisolism and obesity. *Ann NY Acad Sci*. 1995;771:665–676.
2. **Geer EB, Islam J, Buettner C.** Mechanisms of glucocorticoid-induced insulin resistance: focus on adipose tissue function and lipid metabolism. *Endocrinol Metab Clin North Am*. 2014;43:75–102.
3. **Björntorp P.** Body fat distribution, insulin resistance, and metabolic diseases. *Nutrition*. 1997;13:795–803.
4. **Walker BR, Andrew R.** Tissue production of cortisol by 11β-hydroxysteroid dehydrogenase type 1 and metabolic disease. *Ann NY Acad Sci*. 2006;1083:165–184.
5. **Chrousos GP.** The role of stress and the hypothalamic-pituitary-adrenal axis in the pathogenesis of the metabolic syndrome: neuroendocrine and target tissue-related causes. *Int J Obes Relat Metab Disord*. 2000;24(suppl 2):S50–S55.
6. **Collino M.** High dietary fructose intake: sweet or bitter life? *World J Diabetes*. 2011;2:77–81.
7. **Gulati S, Misra A.** Sugar intake, obesity, and diabetes in India. *Nutrients*. 2014;6:5955–5974.
8. **Martinez Calejman C, Di Gruccio JM, Mercau ME, et al.** Insulin sensitization with a peroxisome proliferator-activated receptor γ agonist prevents adrenocortical lipid infiltration and secretory changes induced by a high-sucrose diet. *J Endocrinol*. 2012;214:267–276.
9. **Auvinen HE, Romijn JA, Biermasz NR, et al.** Effects of high fat diet on the basal activity of the hypothalamus-pituitary-adrenal axis in mice: a systematic review. *Horm Metab Res*. 2011;43:899–906.
10. **Tannenbaum BM, Brindley DN, Tannenbaum GS, et al.** High-fat feeding alters both basal and stress-induced hypothalamic-pituitary-adrenal activity in the rat. *Am J Physiol*. 1997;273:E1168–E1177.
11. **McNeilly AD, Stewart CA, Sutherland C, Balfour DJ.** High fat feeding is associated with stimulation of the hypothalamic-pituitary-adrenal axis and reduced anxiety in the rat. *Psychoneuroendocrinology*. 2015;52:272–280.
12. **Hotamisligil GS.** Role of endoplasmic reticulum stress and c-Jun NH2-terminal kinase pathways in inflammation and origin of obesity and diabetes. *Diabetes*. 2005;54(suppl 2):S73–S78.
13. **Ruiz-Ramírez A, Chávez-Salgado M, Peñeda-Flores JA, Zapata E, Masso F, El-Hafidi M.** High-sucrose diet increases ROS generation, FFA accumulation, UCP2 level, and proton leak in liver mitochondria. *Am J Physiol Endocrinol Metab*. 2011;301:E1198–E1207.
14. **Yorimitsu T, Nair U, Yang Z, Klionsky DJ.** Endoplasmic reticulum stress triggers autophagy. *J Biol Chem*. 2006;281:30299–30304.
15. **Bonora E, Moghetti P, Zancanaro C, et al.** Estimates of in vivo insulin action in man: comparison of insulin tolerance tests with euglycemic and hyperglycemic glucose clamp studies. *J Clin Endocrinol Metab*. 1989;68:374–378.
16. **Cymeryng CB, Dada LA, Podestá EJ.** Effect of nitric oxide on rat adrenal zona fasciculata steroidogenesis. *J Endocrinol*. 1998;158:197–203.
17. **Mercau ME, Astort F, Giordanino EF, et al.** Involvement of PI3K/Akt and p38 MAPK in the induction of COX-2 expression by bacterial lipopolysaccharide in murine adrenocortical cells. *Mol Cell Endocrinol*. 2014;384:43–51.
18. **Livak KJ, Schmittgen TD.** Analysis of relative gene expression data using real-time quantitative PCR and the $2(-\Delta\Delta C(T))$ method. *Methods*. 2001;25:402–408.
19. **Gumbiner B, Kelly RB.** Two distinct intracellular pathways trans-

port secretory and membrane glycoproteins to the surface of pituitary tumor cells. *Cell*. 1982;28:51–59.
20. **Kitamura T, Feng Y, Kitamura YI, et al.** Forkhead protein FoxO1 mediates Agrp-dependent effects of leptin on food intake. *Nat Med*. 2006;12:534–540.
21. **Kimura S, Noda T, Yoshimori T.** Dissection of the autophagosome maturation process by a novel reporter protein, tandem fluorescent-tagged LC3. *Autophagy*. 2007;3:452–460.
22. **Shin AC, MohanKumar SM, Sirivelu MP, et al.** Chronic exposure to a high-fat diet affects stress axis function differentially in diet-induced obese and diet-resistant rats. *Int J Obes (Lond)*. 2010;34:1218–1226.
23. **Lomax MA, Karamanlidis G, Laws J, Cremers SG, Weinberg PD, Clarke L.** Pigs fed saturated fat/cholesterol have a blunted hypothalamic-pituitary-adrenal function, are insulin resistant and have decreased expression of IRS-1, PGC1α and PPARα. *J Nutr Biochem*. 2013;24:656–663.
24. **Auvinen HE, Romijn JA, Biermasz NR, et al.** The effects of high fat diet on the basal activity of the hypothalamus-pituitary-adrenal axis in mice. *J Endocrinol*. 2012;214:191–197.
25. **D'Alessandro ME, Selenscig D, Illesca P, Chicco A, Lombardo YB.** Time course of adipose tissue dysfunction associated with antioxidant defense, inflammatory cytokines and oxidative stress in dyslipemic insulin resistant rats. *Food Funct*. 2015;6:1299–1309.
26. **Srividhya S, Ravichandran MK, Anuradha CV.** Metformin attenuates blood lipid peroxidation and potentiates antioxidant defense in high fructose-fed rats. *J Biochem Mol Biol Biophys*. 2002;6:379–385.
27. **Bonnard C, Durand A, Peyrol S, et al.** Mitochondrial dysfunction results from oxidative stress in the skeletal muscle of diet-induced insulin-resistant mice. *J Clin Invest*. 2008;118:789–800.
28. **Holmström KM, Finkel T.** Cellular mechanisms and physiological consequences of redox-dependent signalling. *Nat Rev Mol Cell Biol*. 2014;15:411–421.
29. **Yuzefovych LV, LeDoux SP, Wilson GL, Rachek LI.** Mitochondrial DNA damage via augmented oxidative stress regulates endoplasmic reticulum stress and autophagy: crosstalk, links and signaling. *PLoS One*. 2013;8:e83349.
30. **Ozcan U, Cao Q, Yilmaz E, et al.** Endoplasmic reticulum stress links obesity, insulin action, and type 2 diabetes. *Science*. 2004;306:457–461.
31. **Marek G, Pannu V, Shanmugham P, et al.** Adiponectin resistance and proinflammatory changes in the visceral adipose tissue induced by fructose consumption via ketohexokinase-dependent pathway. *Diabetes*. 2015;64:508–518.
32. **Wang H, Sun RQ, Zeng XY, et al.** Restoration of autophagy alleviates hepatic ER stress and impaired insulin signalling transduction in high fructose-fed male mice. *Endocrinology*. 2015;156:169–181.
33. **Qiu W, Zhang J, Dekker MJ, et al.** Hepatic autophagy mediates endoplasmic reticulum stress-induced degradation of misfolded apolipoprotein B. *Hepatology*. 2011;53:1515–1525.
34. **Høyer-Hansen M, Jäättelä M.** Connecting endoplasmic reticulum stress to autophagy by unfolded protein response and calcium. *Cell Death Differ*. 2007;14:1576–1582.
35. **Bachar-Wikstrom E, Wikstrom JD, Ariav Y, et al.** Stimulation of autophagy improves endoplasmic reticulum stress-induced diabetes. *Diabetes*. 2013;62:1227–1237.
36. **Campbell HM, Khan N, Cone C, Raisch DW.** Relationship between diet, exercise habits, and health status among patients with diabetes. *Res Social Adm Pharm*. 2011;7:151–161.
37. **Wright DW, Hansen RI, Mondon CE, Reaven GM.** Sucrose-induced insulin resistance in the rat: modulation by exercise and diet. *Am J Clin Nutr*. 1983;38:879–883.
38. **Campbell JE, Király MA, Atkinson DJ, D'souza AM, Vranic M, Riddell MC.** Regular exercise prevents the development of hyperglucocorticoidemia via adaptations in the brain and adrenal glands in male Zucker diabetic fatty rats. *Am J Physiol Regul Integr Comp Physiol*. 2010;299:R168–R176.
39. **Lee JS, Pinnamaneni SK, Eo SJ, et al.** Saturated, but not n-6 polyunsaturated, fatty acids induce insulin resistance: role of intramuscular accumulation of lipid metabolites. *J Appl Physiol (1985)*. 2006;100:1467–1474.
40. **Chavez JA, Summers SA.** Characterizing the effects of saturated fatty acids on insulin signaling and ceramide and diacylglycerol accumulation in 3T3-L1 adipocytes and C2C12 myotubes. *Arch Biochem Biophys*. 2003;419:101–109.
41. **Perez I, El Hafidi M, Carvajal K, Baños G.** Castration modifies aortic vasoreactivity and serum fatty acids in a sucrose-fed rat model of metabolic syndrome. *Heart Vessels*. 2009;24:147–155.
42. **Oh YT, Kim J, Kang I, Youn JH.** Regulation of hypothalamic-pituitary-adrenal axis by circulating free fatty acids in male Wistar rats: role of individual free fatty acids. *Endocrinology*. 2014;155:923–931.
43. **Lanfranco F, Giordano R, Pellegrino M, et al.** Free fatty acids exert an inhibitory effect on adrenocorticotropin and cortisol secretion in humans. *J Clin Endocrinol Metab*. 2004;89:1385–1390.
44. **Yan J, Feng Z, Liu J, et al.** Enhanced autophagy plays a cardinal role in mitochondrial dysfunction in type 2 diabetic Goto-Kakizaki (GK) rats: ameliorating effects of (−)-epigallocatechin-3-gallate. *J Nutr Biochem*. 2012;23:716–724.
45. **Cakir I, Cyr NE, Perello M, et al.** Obesity induces hypothalamic endoplasmic reticulum stress and impairs proopiomelanocortin (POMC) post-translational processing. *J Biol Chem*. 2013;288:17675–17688.